

QCD pressure: renormalization group optimized perturbation theory confronts lattice

Jean-Loïc Kneur,^{1,*} Marcus Benghi Pinto,^{2,†} and Tulio E. Restrepo^{2,‡}

¹Laboratoire Charles Coulomb (L2C), UMR 5221 CNRS-Université Montpellier, 34095 Montpellier, France

²Departamento de Física, Universidade Federal de Santa Catarina, 88040-900 Florianópolis, SC, Brazil

The quark contribution to the QCD pressure, P_q , is evaluated up to next-to-leading order (NLO) within the renormalization group optimized perturbation theory (RGOPT) resummation approach. To evaluate the complete QCD pressure we simply add the perturbative NLO contribution from massless gluons to the resummed P_q . Despite of this unsophisticated approximation our results for $P = P_q + P_g$ at the central scale $M \sim 2\pi T$ show a remarkable agreement with lattice predictions for $0.25 \lesssim T \lesssim 1$ GeV. We also show that by being imbued with RG properties, the RGOPT produces a drastic reduction of the embarrassing remnant scale dependence that plagues both standard thermal perturbative QCD and hard thermal loop perturbation theory (HTLpt) applications.

At the fundamental level, strongly interacting matter composed by quarks and gluons is described by the non Abelian theory of quantum chromodynamics (QCD) whose coupling constant, α_s , is predicted to decrease with increasing energies as the system evolves to a regime of asymptotic freedom (AF). This property, together with the other crucial phenomena of confinement and chiral symmetry, has triggered the possibility of studying eventual phase transitions related to (de)confinement and chiral symmetry breaking/restoration in the laboratory through experiments involving heavy ion collisions. On the theoretical side, lattice QCD (LQCD) ab initio simulations have predicted that the deconfinement and chiral symmetry restoration occur via an analytic crossover occurring at a pseudo-critical temperature of order $T_{pc} \simeq 155$ MeV with the baryon chemical potential, μ_B , approaching zero [1]. The region at intermediate T and μ_B values ($T \sim 100$ MeV, $\mu_B \sim 900$ MeV), is currently being explored by experiments such as the beam energy scan at RHIC whose aim is to confirm the existence of a critical end point which locates the end of a first order transition line predicted to start at $T = 0$ [2]. Another region, covering the range $T \sim 0 - 30$ MeV and $\mu_B \gtrsim 1000$ MeV, is essential for the description of compact stellar objects such as neutron stars. Unfortunately, due to the notorious sign problem [3], LQCD encounters a more hostile environment within these two phenomenologically important regions where numerical simulations cannot yet be reliably implemented. Therefore, the development of reliable alternatives with more analytical tools remains timely. Several such alternatives can partly address the deconfinement and/or chiral symmetry restoration, like extensions of the Nambu–Jona-Lasinio (NJL) model[2, 4–6], or with more complete QCD dynamics, the Dyson-Schwinger equations (see e.g. [7, 8]), the functional Renormalization Group [9], or other approaches[10]. Our present approach is rather built on weak-coupling expansion as a starting point in the evaluation of physical observables in powers (and logarithms) of $g = 4\pi\alpha_s$. However, perturbative results require a further resummation to be compatible with strong or

even moderate coupling regimes (see Refs. [11–13] for reviews). At finite temperatures, resumming the perturbative series cure some of the infrared divergences from zero modes, improving also convergence issues (but does not solve the intrinsically nonperturbative infrared issues due to static magnetic fields[14]). An efficient way to perform a resummation is to reorganize the perturbative series around a quasiparticle mass parameter. Such an approach appears in the literature under various names, like optimized perturbation theory (OPT) [15–17], linear δ expansion (LDE) [18], variational perturbation theory (VPT) [19], or in the thermal context, screened perturbation theory (SPT) [20, 21].

Analogous thermal resummations in the QCD gluon sector is far from obvious due to gauge-invariance issues, but had been circumvented by Braaten and Pisarski [22] who proposed a gauge-invariant non-local Lagrangian embedding hard thermal loop (HTL) contributions, Landau damping, and screening gluon thermal mass, with momentum-dependent self-energies and HTL-dressed vertices. The high temperature approximation of HTL could be successfully generalized in the so-called HTL perturbation theory (HTLpt) [23], allowing for the evaluation of the QCD thermodynamics at the NNLO (three-loop), considering both the glue[24] and quark sectors at finite temperatures and baryonic densities [25–27]. The final NNLO results turned out to be in good agreement with LQCD predictions for temperatures down to $T \approx 1.5 T_{pc}$ for the “central” renormalization scale choice $M = 2\pi\sqrt{T^2 + \mu^2/\pi^2}$. Unfortunately this agreement quickly deteriorates as moderate scale variations of a factor 2 induce relative variations of order 1 or more. Moreover it has been observed that this scale dependence strongly *increases* at higher orders, most predominantly from NLO to NNLO. It is important to remark that standard pQCD results are also plagued by a similar growing and strong scale dependence at high orders [11, 28, 29].

More recently an alternative resummation approach has been proposed, the renormalization group optimized perturbation theory (RGOPT) [30–33], that essentially combines a variational mass prescription with embedded

consistent RG invariance properties. Within QCD, at $T = \mu_B = 0$, the method has been used to estimate the coupling α_s , predicting values [33] compatible with the world averages [34]. Still at $T = 0 = \mu$, a precise prediction was obtained for the quark condensate [35, 36]. In thermal theories the RGOPT has been applied, e.g., to the simpler scalar ϕ^4 model [30, 31] at NLO, showing how it improves the generic residual scale dependence as compared to both standard thermal perturbation theory and SPT. Concerning QCD, the direct application of RGOPT to the pure glue sector is however momentarily obstructed by specific technical difficulties, as it involves new types of very involved thermal integrals [37]. Yet at least a nontrivial NLO evaluation of the QCD pressure can be performed in a more simple-minded and relatively easy way, if one considers the case of massive quarks and massless gluons. In this vein we have recently applied the RGOPT to the QCD quark sector only, while considering the gluons to be massless, in order to evaluate the NLO pressure at finite densities and vanishing temperatures [38]. Our NLO results show a good numerical agreement with *higher* order state of the art $\mathcal{O}(g^3 \ln^2 g)$ pQCD predictions, with a visible improvement (although relatively modest for cold matter) of the residual scale dependence. In the present work, we aim to extend the $T = 0, \mu_B \neq 0$ application performed in Ref. [38] in order to consider a thermal bath. Our strategy is to apply our construction to the quark sector which, together with the purely perturbative NLO contribution of massless gluons, will compose our complete NLO QCD pressure: $P(T, \mu_B) = P_q^{RGOPT} + P_g^{PT}$ where $P_g^{PT} \sim T^4$. We believe that the results reported here represent a significant step towards the determination of thermodynamical observables with RG improved properties. Technical details related to our calculation may be found in a companion paper [39].

Our starting point is the perturbative QCD pressure for three quark flavors with degenerate masses, $m_u = m_d = m_s \equiv m$, and massless gluons: $P = P_q^{PT} + P_g^{PT}$. Let us consider first the quark contribution P_q and how the RGOPT is built on it. At NLO ($\mathcal{O}(g)$) the *massive* quark contributions to the pressure can be obtained by combining the vacuum results of Ref. [35] and $T, \mu \neq 0$ results of Refs. [40, 41]. The *per flavor* result reads

$$\begin{aligned} \frac{P_q^{PT}}{N_f N_c} &= -\frac{m^4}{8\pi^2} \left(\frac{3}{4} - L_m \right) + 2T^4 J_1 \\ &- 3g \frac{m^4}{2(2\pi)^4} C_F \left(L_m^2 - \frac{4}{3} L_m + \frac{3}{4} \right) \\ &- g C_F \left\{ \left[\frac{m^2}{4\pi^2} (2 - 3L_m) + \frac{T^2}{6} \right] T^2 J_2 \right. \\ &\left. + \frac{T^4}{2} J_2^2 + m^2 T^2 J_3 \right\}, \end{aligned} \quad (1)$$

where $L_m = \ln(m/M)$, $g \equiv 4\pi\alpha_s(M)$, M is the arbitrary renormalization scale in the $\overline{\text{MS}}$ -scheme, $C_F = (N_c^2 -$

$1)/(2N_c)$, $N_c = 3$, and $N_f = 3$. In-medium and thermal effects are included in the (dimensionless) single integrals:

$$J_1 = \int \frac{d^3\hat{\mathbf{p}}}{(2\pi)^3} \left\{ \ln \left[1 + e^{-(E_p + \frac{\mu}{T})} \right] + \ln \left[1 + e^{-(E_p - \frac{\mu}{T})} \right] \right\}, \quad (2)$$

with $\hat{\mathbf{p}} \equiv \mathbf{p}/T$, $E_p = \sqrt{\hat{\mathbf{p}}^2 + m^2/T^2}$,

$$J_2 = \int \frac{d^3\hat{\mathbf{p}}}{(2\pi)^3} \frac{1}{E_p} [f^+(E_p) + f^-(E_p)], \quad (3)$$

and in the double integral (after angular integration over $p \cdot q/(|p||q|)$)

$$\begin{aligned} J_3 &= \frac{1}{(2\pi)^4} \int_0^\infty \int_0^\infty \frac{d\hat{p} \hat{p} d\hat{q} \hat{q}}{E_p E_q} \left\{ \Sigma_+ \ln \left[\frac{E_p E_q - \frac{m^2}{T^2} - \hat{p}\hat{q}}{E_p E_q - \frac{m^2}{T^2} + \hat{p}\hat{q}} \right] \right. \\ &\left. + \Sigma_- \ln \left[\frac{E_p E_q + \frac{m^2}{T^2} + \hat{p}\hat{q}}{E_p E_q + \frac{m^2}{T^2} - \hat{p}\hat{q}} \right] \right\}, \end{aligned} \quad (4)$$

where $\Sigma_\pm = f^+(E_p) f^\pm(E_q) + f^-(E_p) f^\mp(E_q)$.

The Fermi-Dirac distributions for anti-quarks (+ sign) and quarks (- sign) read

$$f^\pm(E_p) = \frac{1}{1 + e^{(E_p \pm \frac{\mu}{T})}}, \quad (5)$$

where μ is the quark chemical potential, related to the baryonic chemical potential via $\mu_B = 3\mu$. In the present work we consider symmetric quark matter and thus do not distinguish the chemical potentials associated with different flavors ($\mu_s = \mu_u = \mu_d \equiv \mu$). For the quark sector the Stefan-Boltzmann limit is

$$\frac{PSB}{N_c N_f} = T^4 \left(\frac{7\pi^2}{180} \right) \left(1 + \frac{120}{7} \hat{\mu}^2 + \frac{240}{7} \hat{\mu}^4 \right), \quad (6)$$

where $\hat{\mu} = \mu/(2\pi T)$.

Defining the (massive) homogenous RG operator

$$M \frac{d}{dM} = M \partial_M + \beta(g) \partial_g - m \gamma_m(g) \partial_m, \quad (7)$$

note that acting with Eq.(7) on the massive pressure Eq.(1) leaves a non RG-invariant term of *leading order*, $\sim m^4 \ln(M)$. To restore a perturbatively RG-invariant massive pressure, we proceed as in Refs.[30, 31, 35] (or closer to the present case, as in Ref. [38]), subtracting a finite zero point contribution,

$$\frac{P_q^{RGPT}}{N_c N_f} = \frac{P_q^{PT}}{N_c N_f} - \frac{m^4}{g} \sum_k s_k g^k, \quad (8)$$

where the s_i are determined at successive orders so that

$$M \frac{d}{dM} \left(\frac{P_q^{RGPT}}{N_c N_f} \right) = \mathcal{O}(g^2 m^4), \quad (9)$$

up to neglected higher order terms. Our evaluations being carried up to $\mathcal{O}(g)$ it suffices to determine the first

two s_0 and s_1 coefficients. They involve, through Eq.(7), coefficients of the β function and anomalous mass dimension, γ_m , relevant to the $T = \mu = 0$ pressure. Our normalizations are $\beta(g) = -2b_0g^2 - 2b_1g^3 + \mathcal{O}(g^4)$ and $\gamma_m(g) = \gamma_0g + \gamma_1g^2 + \mathcal{O}(g^3)$ where

$$(4\pi)^2 b_0 = 11 - \frac{2}{3}N_f, \quad (10)$$

$$(4\pi)^4 b_1 = 102 - \frac{38}{3}N_f, \quad (11)$$

$$\gamma_0 = \frac{1}{2\pi^2}, \quad (4\pi)^4 \gamma_1 = \frac{404}{3} - \frac{40}{9}N_f. \quad (12)$$

One then finds [35, 38]

$$s_0 = -[(4\pi)^2(b_0 - 2\gamma_0)]^{-1}, \quad (13)$$

$$s_1 = -\frac{1}{4} \left[\frac{b_1 - 2\gamma_1}{4(b_0 - 2\gamma_0)} - \frac{1}{12\pi^2} \right]. \quad (14)$$

Implementing the RGOPT involves the following steps (see for more details e.g. [33, 38, 39]): 1) first one restores (perturbative) RG invariance of the massive pressure, giving Eq.(8) with Eqs.(13),(14) at NLO. 2) The resulting expression is variationally modified, according to the prescription [33, 38]

$$P^{RGPT}(m \rightarrow m(1 - \delta)^a, g \rightarrow \delta g) \equiv P^{RGOPT}, \quad (15)$$

acting thus in the present case on Eq.(8). 3) Next one reexpands (15) in powers of δ , setting $\delta \rightarrow 1$ to recover the massless case. We stress that m is now an arbitrary variational mass parameter, to be fixed by a sensible prescription explicited below. 4) At this stage one also needs to fix the exponent a introduced in Eq.(15), whose role is crucial for RG consistency in our framework. Expanding to LO, $\mathcal{O}(\delta^0)$, and requiring the resulting pressure to satisfy the *reduced* (massless) RG equation:

$$[M\partial_M + \beta(g)\partial_g] P_q^{RGOPT} = 0, \quad (16)$$

leads to $a = \gamma_0/(2b_0)$ [33, 35, 38]. At higher orders, we keep for simplicity the same prescription, which has extra advantages as explained below. The resulting NLO RGOPT-modified pressure after steps 1)–4) reads

$$\begin{aligned} \frac{P_q^{RGOPT}}{N_f N_c} &= -\frac{m^4}{8\pi^2} \left(\frac{3}{4} - L_m \right) + 2T^4 J_1 \\ &+ \frac{m^4}{(2\pi)^2} \left(\frac{\gamma_0}{b_0} \right) \left(\frac{1}{2} - L_m \right) + m^2 \left(\frac{\gamma_0}{b_0} \right) T^2 J_2 \\ &- 3g \frac{m^4}{2(2\pi)^4} C_F \left(L_m^2 - \frac{4}{3}L_m + \frac{3}{4} \right) \\ &- g C_F \left\{ \left[\frac{m^2}{4\pi^2} (2 - 3L_m) + \frac{T^2}{6} \right] T^2 J_2 \right. \\ &\left. + \frac{T^4}{2} J_2^2 + m^2 T^2 J_3 \right\} \end{aligned}$$

$$\begin{aligned} &+ \frac{m^4}{(4\pi)^2 b_0} \left\{ \frac{1}{g} \left(1 - \frac{\gamma_0}{b_0} \right) \right. \\ &\left. + \left[(b_1 - 2\gamma_1)\pi^2 - \frac{(b_0 - 2\gamma_0)}{3} \right] \right\}. \quad (17) \end{aligned}$$

At NLO, Eq.(16) with $a = \gamma_0/(2b_0)$ is no longer exactly satisfied, thus giving an independent constraint. Accordingly in contrast with OPT/SPT the remnant m can be fixed in two different manners[30, 31, 38]. Either, from using a standard stationarity criterion[15], the mass optimization prescription (MOP):

$$\left. \frac{\partial P_q^{RGOPT}}{\partial m} \right|_{\bar{m}} \equiv 0, \quad (18)$$

or alternatively from Eq.(16). The coupling $g(M)$ is determined from standard PT two-loop running, with renormalization scale M chosen as a multiple of πT as usual. At NLO $P_q^{RGOPT}(\bar{m}(g))$ inevitably has a remnant scale dependence, basically because the subtractions in Eq.(8) solely guarantee RG invariance up to remnant higher order terms. But it is a nontrivial consequence of our subsequent construction, mainly Eq.(15), that this remnant dependence remains moderate, of order $m^4 g^2$ at NLO, as will be illustrated below. However, regarding Eq.(17), both Eq.(18) and Eq.(16) fail to give a real dressed mass $\bar{m}(g, T, \mu)$ for a substantial part of the physically relevant T, μ range. The occurrence of non-unique solutions at higher orders, some being complex, is a well-known burden with OPT/SPT approaches. In contrast $a = \gamma_0/(2b_0)$ in Eq.(15) guarantees that the only acceptable solutions are those matching [33] the asymptotic freedom (AF) behavior for $g \rightarrow 0$ at $T = 0$, a compelling criterion that often selects a unique solution. In addition the nonreal solution issue can be cured in an RG consistent manner by performing a renormalization scheme change (RSC)[33, 38, 39]. With this aim we define a RSC acting only on the variational mass in our framework,

$$m \rightarrow m'(1 + B_2 g^2), \quad (19)$$

where a single B_2 parametrizes a NLO RSC from the original $\overline{\text{MS}}$ -scheme. The latter induces an extra term $-4gm^4 s_0 B_2$ in Eq.(1) (renaming afterwards $m' \rightarrow m$ the variational mass to avoid excessive notation changes), entering thus the MOP Eq.(18) and RG Eq.(16). Now since we aim to solve the latter for exact m and g dependence, Eq.(19) modifies those purposefully, when now considered as constraints for the arbitrary mass m after the (all order) modifications induced from Eq.(15). Accordingly B_2 may be considered an extra variational parameter, quite similarly to m , thus to be fixed by a sensible prescription.

Considering specifically the RG Eq.(16), it can be conveniently written as a quadratic form in $\ln(m^2/M^2)$,

$$-\ln \frac{m^2}{M^2} + B_{rg} \mp \frac{8\pi^2}{g} \sqrt{\frac{2}{3} D_{rg}} = 0, \quad (20)$$

where explicitly

$$B_{rg} = -\frac{1}{b_0 g} + \frac{172}{81} - \frac{64}{81} \left(\frac{4g}{9\pi^2} \right) \frac{1}{1 + \frac{4g}{9\pi^2}} + 8\pi^2 \frac{T^2}{m^2} J_2, \quad (21)$$

$$D_{rg} = -\frac{g(4g + 81\pi^2)}{27(4g + 9\pi^2)^2} - g^2 \left(\frac{3}{7} B_2 + \frac{11}{384\pi^4} \right) + g^2 \frac{T^4}{m^4} J_2 \left(J_2 - \frac{1}{6} \right) - g^2 \frac{T^2}{m^2} J_3. \quad (22)$$

Note that a quite similar quadratic form can be obtained for the MOP Eq.(18), with its specific expressions $B_{rg} \rightarrow B_{mop}$, $D_{rg} \rightarrow D_{mop}$ [39]. As above anticipated, in the original $\overline{\text{MS}}$ -scheme ($B_2 = 0$) one can have $D_{rg} < 0$ (or similarly $D_{mop} < 0$) in some physically relevant parameter ranges due to some negative contributions, leading thus to nonreal NLO $\overline{m}(T, \mu)$ solutions. Accordingly to recover real solutions in a large range, while at the same time fulfilling the crucial AF-matching requirement, the comprehensive analysis performed in Ref. [39] suggests the following prescriptions: The arbitrary RSC parameter B_2 is fixed by partly (respectively fully) cancelling D_{mop} (respectively D_{rg}). For the RG prescription explicitly

$$D_{rg}(B_2) = 0 \quad (23)$$

fixes B_2 using Eq.(22). It gives a single real solution for \overline{m} , determined by the first two terms of Eq.(20), the latter being still an implicit equation in m for $T, \mu \neq 0$ via J_2 entering Eq.(21). The prescription Eq.(23) may be seen at first as a rather peculiar choice, but there happens to be very few other possible prescriptions to recover a real RG solution. Note that the resulting $\overline{m}(B_2)$ still involves arbitrary higher order contributions, as well as nontrivial T, μ dependence via B_{rg} in Eq.(21). A similar analysis holds for the MOP Eq.(18), but leading to a \overline{m} having quite different properties (we refer to Ref.[39] for details). We stress that for the two prescriptions the resulting $\overline{m}(B_2)$ is an intermediate variational parameter without much physical meaning outside its use in the pressure. As illustrated below both prescriptions give drastically reduced remnant scale dependence as compared to pQCD, but the best results are obtained from the RG prescription Eqs.(20),(23). This is not very surprising as the latter more directly embeds RG properties as compared to Eq.(18). However for more complete and conservative coverage of the possible variants at NLO, we will illustrate both RG and MOP prescription results below.

Coming to the full QCD pressure, we simply add to Eq.(17) the NLO glue contributions [42],

$$P_g^{PT} = \frac{8\pi^2}{45} T^4 \left[1 - \frac{15}{(4\pi)^2} g \right]. \quad (24)$$

Thus we can now compare the NLO RGOPT full QCD results with those from HTLpt [25, 27] and (massless)

pQCD [28], as well as with available LQCD data from Refs. [43–45]. For the numerical evaluations of NLO quantities we take the exact two-loop running coupling (see, e.g., Ref. [38]) obtained by solving for $g(M)$

$$\ln \frac{M}{\Lambda_{\overline{\text{MS}}}} = \frac{1}{2b_0 g} + \frac{b_1}{2b_0^2} \ln \left(\frac{b_0 g}{1 + \frac{b_1}{b_0} g} \right), \quad (25)$$

for a given $\Lambda_{\overline{\text{MS}}}$ value (this also defines $\Lambda_{\overline{\text{MS}}}$ at two-loop level in our conventions). We take $\Lambda_{\overline{\text{MS}}} = 335$ MeV for $N_f = 3$, which is very close to the latest world average value[34]. Notice that, for consistency the NNLO HTLpt[27] and $\mathcal{O}(g^3 \ln g)$ pQCD[28] numerical results reproduced here have been obtained rather with a three-loop order running coupling.

Fig. 1 shows the RGOPT QCD pressure normalized

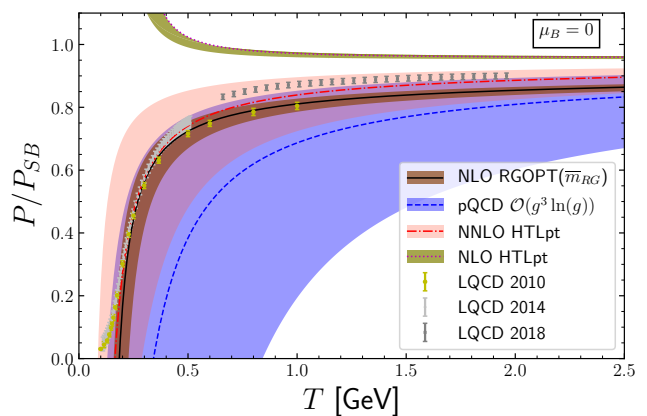


FIG. 1. NLO RGOPT (RG prescription) plus NLO P_g^{PT} pressure (brown band) compared to N³LO $g^3 \ln g$ pQCD (light blue band), NLO HTLpt (light green band) and NNLO HTLpt (light red band), with scale dependence $\pi T \leq M \leq 4\pi T$, and to lattice data [43–45] at $\mu_B = 0$.

by $P_{SB} \equiv P_{SB}^q + P_{SB}^g$ as a function of T for $\mu_B = 0$, obtained with our best RG prescription, Eqs.(20),(23). One notices that for $T \gtrsim 0.25$ GeV our results display a remarkable agreement with the LQCD data of [43] all the way up to $T = 1$ GeV (the highest value considered in those simulations), as well as a very good agreement with more recent LQCD data [44] at intermediate T . Furthermore the RGOPT results are drastically more stable than pQCD and HTLpt when M is varied, as clearly indicated by the different band widths associated to the different approximations. The NLO RGOPT results at central scale, $M = 2\pi T$, observe a better agreement with LQCD data from [43] than NNLO HTLpt for $0.5 \text{ GeV} \lesssim T \lesssim 1 \text{ GeV}$, while the latter lies closer to the higher T data of [45] as compared to RGOPT, showing sizeable differences. A concomitant feature however is the visible tension between low [43] and higher T [45] LQCD data in their common range [NB we show only statistical uncertainties for LQCD, as given in publically available

files[43–45]]. In Fig. 1 one also notices that HTLpt at NLO and pQCD at $\mathcal{O}(g^3 \ln g)$ are still far from lattice data, moreover the NLO HTLpt stays close to SB limit at intermediate to low temperatures. We further mention that while the RGOPT band width illustrated correctly reflects the *total* remnant scale uncertainty resulting from both the (RG resummed) $P_q(M)$ and (standard perturbative) NLO P_g , the *sole* $P_q(M)$ uncertainty would be roughly comparable [39] to the lattice error bars for $T \gtrsim 0.5$ GeV.

Next for completeness in Fig. 2 similar results are shown for the other possible MOP prescription Eq.(18), compared to lattice data and highest order pQCD. As anticipated this prescription is somewhat less efficient than the RG one, regarding the remnant scale uncertainty as well as lattice data comparisons. Yet with respect to pQCD or to (NLO) HTLpt, overall it also appears as a sharp improvement, keeping in mind our NLO approximation.

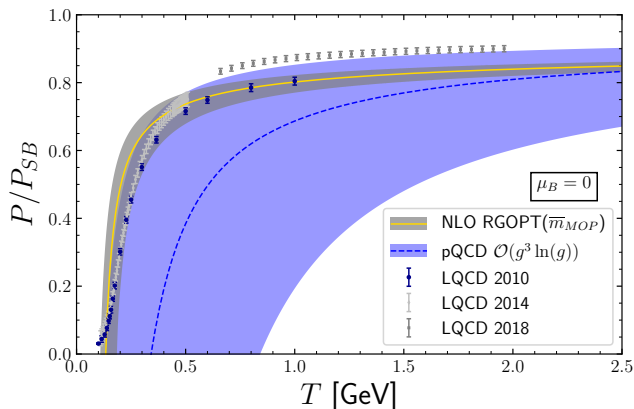


FIG. 2. NLO RGOPT (MOP prescription) plus NLO P_g^{PT} pressure as function of T at $\mu_B = 0$ (grey band) compared to $N^3LO g^3 \ln g$ pQCD (light blue band), with scale dependence $\pi T \leq M \leq 4\pi T$, and to lattice data [43–45].

Another physically interesting quantity is the interaction measure, $\Delta = \mathcal{E} - 3P$, [or at $\mu_B = 0$ equivalently $\Delta = T^5 \partial(P/T^4)/\partial T$, since $\mathcal{E} = -P + ST$ with $S = \partial P/\partial T$ representing the entropy density]. In Fig. 3 the NLO RGOPT interaction measure at $\mu_B = 0$, obtained by a numerical derivative from our best RG prescription above, are compared to the available LQCD data [43–45]. At temperatures $0.3 \text{ GeV} \lesssim T \lesssim 1 \text{ GeV}$ a very good agreement is observed. However, similarly to pQCD and HTLpt, NLO RGOPT as applied here does not describe correctly the peak region near the pseudo-critical T_c temperature as exhibited by lattice data.

Conclusions. In this work we have compared RGOPT predictions regarding the QCD pressure with lattice data for the first time. Our NLO predictions for the central scale, $M = 2\pi T$, turned out to compare very well for temperatures starting at $T \simeq 0.25$ GeV which lies within

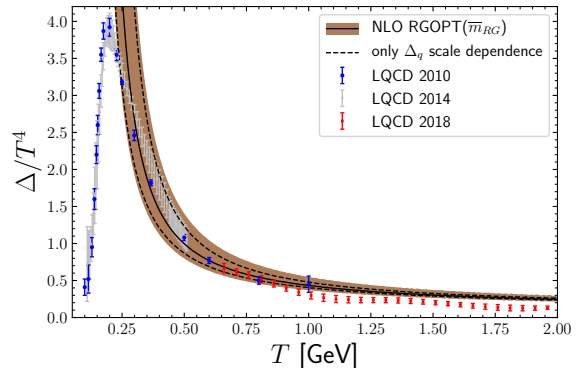


FIG. 3. NLO RGOPT (RG prescription) trace anomaly $\Delta \equiv \mathcal{E} - 3P$, including NLO Δ_g^{PT} (brown band), compared to lattice data [43–45]. The additional dashed lines illustrate the scale uncertainty originating solely from RGOPT quark contributions within the full scale uncertainty added by Δ_g^{PT} (brown) band.

the relatively strong coupling regime ($\alpha_s \simeq 0.3$). This agreement persists up to $T = 1 \text{ GeV}$, the highest value for the LQCD data of [43]. Furthermore, comparing our NLO results with those from NNLO HTLpt one observes that the consistent RG invariance properties native to the RGOPT are drastically attenuating the remnant scale dependence issue. While the striking agreement with lattice data of [43] in Fig. 1 may be partly numerically accidental, variants of our prescription in Fig. 2 still appear in very good agreement given our essentially NLO-based construction, as compared to the state-of-the-art perturbative higher order QCD. The differences of our results with higher $1 \text{ GeV} \lesssim T \lesssim 2 \text{ GeV}$ LQCD data[45] are however visible. Incidentally the LQCD results in [43] and in [45] appear to be in tension in their common range, while the trace anomaly shows more continuity, a feature that may call for more investigations independently of our results. Regarding the comparisons with $2 + 1$ flavor LQCD here illustrated, one may also keep in mind our presently not fully realistic approximation of $N_f = 3$ degenerate flavors. We recall moreover that owing to present technical difficulties in readily applying our approach to the gluon sector, it is included as a purely perturbative NLO contribution on top of the variationally resummed quark contributions. While this simple prescription appears to describe fairly well the moderate to high- T regimes $T \gtrsim 0.25 \text{ GeV} \sim 1.5 T_{pc}$, beyond NLO one could not avoid to face the well-known infrared divergences from gluon contributions, calling for appropriate resummations. Finally we mention that the NLO RG-improved properties exhibited here extend without degradation to sizeable chemical potential values (for illustrations we refer to our companion paper [39]). The latter indicate the potential of our approach towards a more systematic exploration of both hot and dense QCD.

Acknowledgments: We thank P. Petreczky for bringing the results of Ref. [45] to our attention. M.B.P. and T.E.R. are partially supported by Conselho Nacional de Desenvolvimento Científico e Tecnológico (CNPq-Brazil) and by Coordenação de Aperfeiçoamento de Pessoal de Nível Superior-(CAPES-Brazil)-Finance Code 001. This work was also financed in part by INCT-FNA (Process No. 464898/2014-5).

* jean-loic.kneur@umontpellier.fr

† marcus.benghi@ufsc.br

‡ tulio.restrepo@posgrad.ufsc.br

- [1] Y. Aoki, G. Endrodi, Z. Fodor, S. D. Katz and K. K. Szabo, *Nature* **443**, 675 (2006); Y. Aoki, S. Borsanyi, S. Durr, Z. Fodor, S. D. Katz, S. Krieg and K. K. Szabo, *JHEP* **06**, 088 (2009); S. Borsanyi *et al.* [Wuppertal-Budapest], *JHEP* **09**, 073 (2010); A. Bazavov, T. Bhattacharya, M. Cheng, C. DeTar, H. T. Ding, S. Gottlieb, R. Gupta, P. Hegde, U. M. Heller and F. Karsch, *et al.* *Phys. Rev. D* **85**, 054503 (2012).
- [2] M. Buballa, *Phys. Rept.* **407**, 205 (2005).
- [3] P. de Forcrand, *PoS LAT* **2009**, 010 (2009); G. Aarts, *J. Phys. Conf. Ser.* **706**, 022004 (2016).
- [4] P. Costa, M. C. Ruivo and C. A. de Sousa, *Phys. Rev. D* **77**, 096001 (2008) [arXiv:0801.3417 [hep-ph]].
- [5] K. Fukushima, *Phys. Lett. B* **591**, 277-284 (2004) [arXiv:hep-ph/0310121 [hep-ph]].
- [6] P. Costa, M. C. Ruivo, C. A. de Sousa and H. Hansen, *Symmetry* **2**, 1338-1374 (2010) [arXiv:1007.1380 [hep-ph]].
- [7] C. D. Roberts and S. M. Schmidt, *Prog. Part. Nucl. Phys.* **45**, S1-S103 (2000) [arXiv:nucl-th/0005064 [nucl-th]].
- [8] C. S. Fischer, *Prog. Part. Nucl. Phys.* **105**, 1-60 (2019) [arXiv:1810.12938 [hep-ph]].
- [9] W. j. Fu, J. M. Pawłowski and F. Rennecke, *Phys. Rev. D* **101**, no.5, 054032 (2020) [arXiv:1909.02991 [hep-ph]]; F. Gao and J. M. Pawłowski, *Phys. Rev. D* **102**, no.3, 034027 (2020) [arXiv:2002.07500 [hep-ph]].
- [10] J. Maelger, U. Reinosa and J. Serreau, *Phys. Rev. D* **97**, no.7, 074027 (2018) [arXiv:1710.01930 [hep-ph]].
- [11] J. P. Blaizot, E. Iancu and A. Rebhan, In *Hwa, R.C. (ed.) *et al.*: Quark gluon plasma* 60-122 [hep-ph/0303185]; U. Kraemmer and A. Rebhan, *Rept. Prog. Phys.* **67**, 351 (2004).
- [12] M. Laine and A. Vuorinen, *Lect. Notes Phys.* **925**, 1 (2016).
- [13] J. Ghiglieri, A. Kurkela, M. Strickland and A. Vuorinen, *Phys. Rept.* **880**, 1 (2020).
- [14] A. D. Linde, *Phys. Lett. B* **96**, 289-292 (1980)
- [15] P.M. Stevenson, *Phys. Rev. D* **23**, 2916 (1981); *Nucl. Phys. B* **203**, 472 (1982).
- [16] A. Okopinska, *Phys. Rev. D* **35**, 1835-1847 (1987) doi:10.1103/PhysRevD.35.1835;
- [17] H. Yamada, *Z. Phys. C* **59**, 67-76 (1993) doi:10.1007/BF01555840
- [18] A. Duncan and M. Moshe, *Phys. Lett. B* **215**, 352-358 (1988) doi:10.1016/0370-2693(88)91447-5; H. F. Jones and M. Moshe, *Phys. Lett. B* **234**, 492-496 (1990) doi:10.1016/0370-2693(90)92045-K .
- [19] R. P. Feynman and H. Kleinert, *Phys. Rev. A* **34**, 5080 (1986); H. Kleinert, *Phys. Rev. D* **57**, 2264 (1998); *Phys. Lett. B* **434**, 74 (1998); *Phys. Rev. D* **60**, 085001 (1999); *Mod. Phys. Lett. B* **17**, 1011 (2003).
- [20] F. Karsch, A. Patkos and P. Petreczky, *Phys. Lett. B* **401**, 69 (1997); S. Chiku and T. Hatsuda, *Phys. Rev. D* **58**, 076001 (1998); J. O. Andersen, E. Braaten and M. Strickland, *Phys. Rev. D* **63**, 105008 (2001); J. O. Andersen and M. Strickland, *Phys. Rev. D* **64**, 105012 (2001); J. O. Andersen and M. Strickland, *Annals Phys.* **317**, 281 (2005).
- [21] J. O. Andersen and L. Kyllingstad, *Phys. Rev. D* **78**, 076008 (2008) [arXiv:0805.4478 [hep-ph]].
- [22] E. Braaten and R. D. Pisarski, *Phys. Rev. D* **45**, 1827 (1992).
- [23] J. O. Andersen, E. Braaten and M. Strickland, *Phys. Rev. Lett.* **83**, 2139 (1999); J. O. Andersen, E. Braaten and M. Strickland, *Phys. Rev. D* **61**, 074016 (2000).
- [24] J. O. Andersen, M. Strickland and N. Su, *Phys. Rev. Lett.* **104**, 122003 (2010); *JHEP* **1008**, 113 (2010).
- [25] N. Haque, M. G. Mustafa and M. Strickland, *Phys. Rev. D* **87**, 105007 (2013).
- [26] J. O. Andersen, L. E. Leganger, M. Strickland and N. Su, *JHEP* **1108**, 053 (2011); S. Mogliacci, J. O. Andersen, M. Strickland, N. Su and A. Vuorinen, *JHEP* **1312**, 055 (2013); N. Haque, J. O. Andersen, M. G. Mustafa, M. Strickland and N. Su, *Phys. Rev. D* **89**, 061701 (2014).
- [27] N. Haque, A. Bandyopadhyay, J. O. Andersen, M. G. Mustafa, M. Strickland and N. Su, *JHEP* **1405**, 027 (2014).
- [28] K. Kajantie, M. Laine, K. Rummukainen and Y. Schroder, *Phys. Rev. D* **67**, 105008 (2003).
- [29] A. Vuorinen, *Phys. Rev. D* **68**, 054017 (2003).
- [30] J. L. Kneur and M. B. Pinto, *Phys. Rev. D* **92**, 116008 (2015).
- [31] J. L. Kneur and M. B. Pinto, *Phys. Rev. Lett.* **116**, 031601 (2016).
- [32] J. L. Kneur and A. Neveu, *Phys. Rev. D* **81**, 125012 (2010).
- [33] J. L. Kneur and A. Neveu, *Phys. Rev. D* **88**, 074025 (2013).
- [34] M. Tanabashi *et al.* [Particle Data Group], *Phys. Rev. D* **98**, 030001 (2018).
- [35] J. L. Kneur and A. Neveu, *Phys. Rev. D* **92**, 074027 (2015).
- [36] J. L. Kneur and A. Neveu, *Phys. Rev. D* **101**, 074009 (2020).
- [37] J. L. Kneur and M. B. Pinto; in preparation.
- [38] J. L. Kneur, M. B. Pinto and T. E. Restrepo, *Phys. Rev. D* **100**, 114006 (2019)
- [39] J. L. Kneur, M. B. Pinto and T. E. Restrepo, "Renormalization group improved pressure for hot and dense quark matter", arXiv:2101.08240.
- [40] J. I. Kapusta and C. Gale, "*Finite-temperature field theory: Principles and applications*" (Cambridge University Press, 2006).
- [41] M. Laine and Y. Schröder, *Phys. Rev. D* **73**, 085009 (2006).
- [42] E. V. Shuryak, *Sov. Phys. JETP* **47**, 212 (1978); S. A. Chin, *Phys. Lett. B* **78**, 552 (1978).
- [43] S. Borsanyi, G. Endrodi, Z. Fodor, A. Jakovac, S. D. Katz, S. Krieg, C. Ratti and K. K. Szabo, *JHEP* **11**, 077 (2010).
- [44] S. Borsanyi, Z. Fodor, C. Hoelbling, S. D. Katz, S. Krieg

and K. K. Szabo, Phys. Lett. B **730**, 99-104 (2014).

[45] A. Bazavov, P. Petreczky and J. H. Weber, Phys. Rev. D **97**, no.1, 014510 (2018).